



# Fluorescence and photophysical properties of D- $\pi$ -A push-pull systems featuring a 4,5-dicyanoimidazole unit

Miloš Nepraš<sup>a</sup>, Numan Almonasy<sup>a,\*</sup>, Filip Bureš<sup>a</sup>, Jiří Kulhánek<sup>a</sup>, Miroslav Dvořák<sup>b</sup>, Martin Michl<sup>b</sup>

<sup>a</sup> Institute of Organic Chemistry and Technology, Faculty of Chemical Technology, University of Pardubice, Studentská 573, CZ-532 10 Pardubice, Czech Republic

<sup>b</sup> Department of Physical Electronics, Faculty of Nuclear Sciences and Physical Engineering, Czech Technical University in Prague, V Holešovičkách 2, CZ-180 00 Prague, Czech Republic

## ARTICLE INFO

### Article history:

Received 6 December 2010

Received in revised form

25 February 2011

Accepted 17 March 2011

Available online 25 March 2011

### Keywords:

Dicyanoimidazole

Chromophores

Absorption

Fluorescence

Quantum yield

Push-pull

## ABSTRACT

Absorption and fluorescence spectra and fluorescence quantum yields of 18 D- $\pi$ -A push-pull compounds were measured. The investigated chromophores consist of 4,5-dicyanoimidazole — bearing donor — substituted and systematically extended  $\pi$ -conjugated spacers. The influence of temperature and solvent polarity on the spectral and photophysical properties was investigated. Employing INDO/S calculations, the structure–property relationships were discussed.

© 2011 Elsevier Ltd. All rights reserved.

## 1. Introduction

$\pi$ -Conjugated organic molecules end-capped with electron donating and accepting groups attract much attention due to their prospective application as efficient materials in organic electronics and optoelectronics [1]. Therefore, extensive efforts have been focused on the design, synthesis and properties of new electron-accepting systems. High interest has been focused on the synthesis, spectral and photophysical characteristics of 4,5-dicyanoimidazole as new promising acceptor moiety [2]. Recently, Shin et al. [3] reported the synthesis, spectral and photophysical properties and application of series of electron-acceptor conjugated compounds prepared by the Heck coupling of 2-vinyl-4,5-dicyanoimidazole (vinazene) with selected haloaromatics 4,5-Dicyanoimidazole moiety was also incorporated into terephthalic homopolyester [4] and methacrylate copolymer [5]. Thermal and optical characteristics of prepared chromophores were investigated.

Optical properties of the push–pull molecules depend mainly on the polarizability of the electrons localized in  $\pi$ -bonding molecular orbitals [6,7]. Although the polarizability of a molecule is mainly given by its chemical structure, in particular by the length and the structure of the  $\pi$ -conjugated spacer and the electronic

nature of the donors and acceptors attached [8,9], it can also be affected by external factors such as temperature and the solvent used for measurements.

Recently, we have published the design, synthesis, characterization and properties of new family of push-pull  $\pi$ -conjugated molecules featuring 4,5-dicyanoimidazole (DCI) as an acceptor moiety [10,11] and their structural analogues based on 4,5-bis(*N,N*-dimethylanilino)imidazole [12]. The basic UV/Vis, electrochemical and solid state properties were investigated. These heterocyclic Y-shaped compounds proved to be efficient charge-transfer chromophores with prospective application in optoelectronics, optical data storage devices or functional polymers [13].

In the present work, we report spectral UV–Vis absorption and fluorescence characteristics and photophysical properties as well as their dependence on the solvent polarity, temperature and structure of 4,5-dicyanoimidazole chromophore **1–6** prepared as three series **a–c**. Whereas the first, reference, series **a** is unsubstituted ( $R = H$ ), chromophores in the series **b** ( $R = OMe$ ) and **c** ( $R = NMe_2$ ) are end-capped with electron donating methoxy and *N,N*-dimethylamino groups (Fig. 1). In addition, the measured absorption characteristics were further correlated with INDO/S theoretical results.

## 2. Experimental

The synthesis and full spectral characterization of chromophores **1–6** was reported elsewhere [10].

\* Corresponding author. Tel.: +420 466 038 500; fax: +420 466 038 004.

E-mail address: [numan.almonasy@upce.cz](mailto:numan.almonasy@upce.cz) (N. Almonasy).

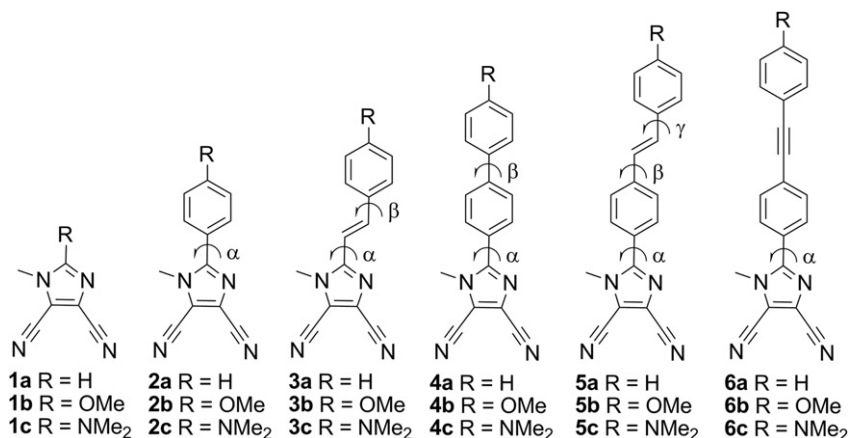


Fig. 1. Molecular structures of investigated chromophores 1–6.

The used solvents, ethyl acetate (EtAc), acetonitrile (MeCN), dibutyl ether (DBE), and 2-Methyltetrahydrofuran (2-MTHF), were spectroscopic grade (Sigma–Aldrich). The absorption spectra were measured on a Perkin Elmer Lambda 35 UV/VIS Spectrophotometer. The fluorescence spectra were measured on a Hitachi Perkin Elmer LS 55 Spectrofluorimeter. As the fluorescence maxima of the investigated compounds are located in a broad wavelength range (320–550 nm), the following fluorescence standards were used for the determination of the fluorescence quantum yields: 1-naphthylamin in cyclohexane ( $\lambda_{\text{max}}^{\text{F}} = 370$  nm,  $q_{\text{F}} = 0.46$ ) [14], quinine sulphate in 0.5 mol/L H<sub>2</sub>SO<sub>4</sub> ( $\lambda_{\text{max}}^{\text{F}} = 445$  nm,  $q_{\text{F}} = 0.54$ ) [15] and coumarin 153 in ethanol ( $\lambda_{\text{max}}^{\text{F}} = 536$  nm,  $q_{\text{F}} = 0.38$ ) [16]. The low temperature fluorescence emission and excitation spectra were measured on an LS55 Spectrofluorimeter equipped with commercial low temperature accessory and special cells. The fluorescence anisotropy measurements were performed on an Edinburgh Analytical Instruments – EAI FS/FL900 spectrofluorimeter equipped with electronically driven Glen-Thompson excitation and emission polarizers. 2-Methyltetrahydrofuran obtained from Merck Chemicals was used for the anisotropy measurements. It was purified by 2 h reflux with potassium hydroxide and final distillation from fresh potassium hydroxide. The chromophore solutions were cooled to 130 K using the Oxford Instruments OptistatDN cryostat head.

### 3. Theoretical

The equilibrium conformations of 1–6 in electronic ground and excited states have been calculated using semiempirical AM1 and INDO/S methods as implemented in WinMOPAC 2.0 Package and using ZINDO/CI method implemented in ArgusLab 4.0 [17].

## 4. Results and discussion

### 4.1. Absorption spectra

The absorption spectra of the compounds within the spectral range of 250–450 nm feature one or two (3c, 5c and 6c) broad absorption bands (Figs. 2–7). Moving from the hydrogen-substituted series **a** to the donor-substituted chromophores in the series **b** and **c**, the longest-wavelength absorption band shifts bathochromically. This bathochromic shift reflects electron donating ability of both substituents and, therefore, the largest shift was observed for *N,N*-dimethylamino-substituted chromophores (series **a**, 40–75 nm). In general, chromophores **3** showed the most

bathochromically shifted longest-wavelength absorption maxima. These results demonstrate a CT character of the first absorption band accompanied with an electron transition from the donor substituent to the electron-acceptor DCI moiety. The relation between the  $\lambda_{\text{max}}^{\text{A}}$  values and  $\pi$ -linkage length and structure was found to be in the order of **5** > **3** > **6** > **4** > **2** in DBE and **3** ≥ **5** > **6** > **4** > **2** in more polar solvents such as EtAc and MeCN. This observation is in agreement with our previous findings [10].

No influence or even small hypsochromic shifts of the absorption maxima with increasing solvent polarity were observed for all studied chromophores (Table 1). The INDO/S calculations indicated that the dipole moments of the ground states of all chromophores in the series **a** and chromophores **2b** and **3b** are lower than that of the vertically formed  $\pi\pi^*$  states. Therefore, equilibrium solvent polarization induced by ground-state dipole moment of these compounds interacts more favourably with ground-state dipole moment than with that of vertical  $\pi\pi^*$  excited state. Consequently, the ground-state is solvated in a greater extent than the excited state and the absorption maxima are more or less shifted hypsochromically with the increasing solvent polarity. This interpretation is in

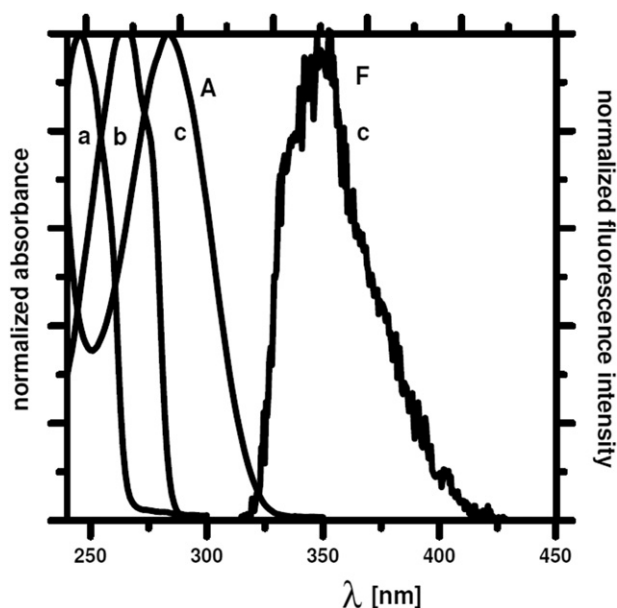


Fig. 2. Absorption (A) and fluorescence (F) spectra of 1a–c in DBE.

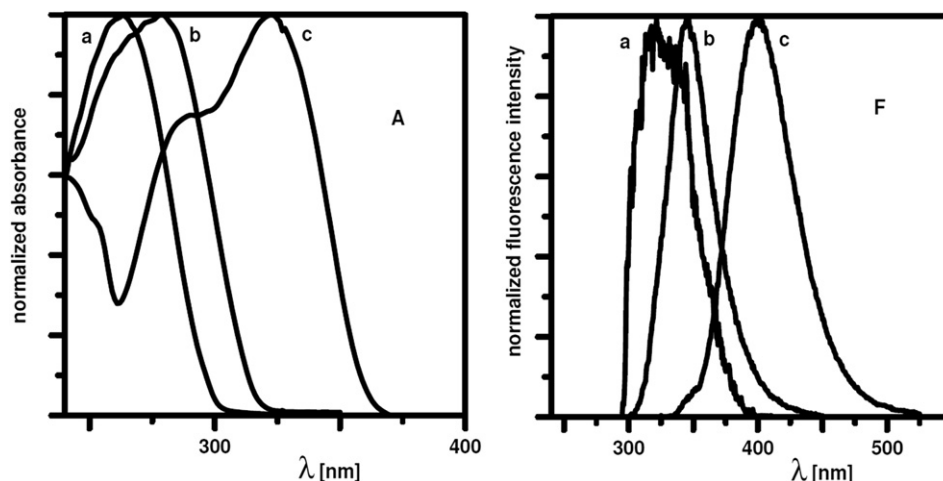


Fig. 3. Absorption (A) and fluorescence (F) spectra of **2a–c** in DBE.

accordance with the experimental absorption maxima of all chromophores in the series **a** and chromophores **2b** and **3b**. As the dipole moments of  $S_1(\pi\pi^*)$  excited states of chromophores **4b**, **5b**, **6b** and all chromophores in the series **c** are larger than that of the ground-states (Table 5), we could expect a greater solvation of the vertical  $\pi\pi^*$  excited state and a bathochromic shift of the absorption maxima in polar solvents. However, no shift or even small hypsochromic shift were found with the increasing solvent polarity.

According to the relation  $\tilde{\nu}_a = \tilde{\nu}_0 + \Delta E_g + \Delta E_e - \Delta E_e$ , where  $\tilde{\nu}_0$  means the vacuum value of the absorption maximum,  $\Delta E_g$  and  $\Delta E_e$  are the stabilization energies of the ground and excited states, respectively.  $\Delta E_e$  means the Franck-Condon destabilization energy [18] of the excited state, i.e. the energy difference between the populated FC vibronic state and zero-point level of the equilibrium nuclear configuration of the excited state. The blue shift of the absorption band takes place when  $\Delta E_g + \Delta E_e > \Delta E_e$ ; this condition is always accomplished when  $\Delta E_g > \Delta E_e$ . However, a hypsochromic shift could also be expected in the case even when  $\Delta E_g < \Delta E_e$ . This depends on  $\Delta E_e$  whose magnitude depends on position of minimum of excited state potential energy surface and on its shape. Moreover, calculated dipole moments of vertically formed  $S_1(\pi\pi^*)$  states of these chromophores are displaced by 13–38° from the direction of the ground-state dipole. Hence, the solvent polarization induced by the ground-state dipole is not aligned to effectively solvate the larger excited-state dipole. These facts could contribute to the slight negative solvatochromism of chromophores in the series **c**.

Absorption spectra of the fluorescent chromophores resemble the fluorescence excitation spectra in the used solvents.

Generally, a lowering of temperature may cause a bathochromic shift of an absorption band owing to an increase of solvent density and consequently of dispersion forces that are responsible for the spectral shifts. At the same time, a lowering of temperature may bring about a hypsochromic shift that can be attributed to changes of spectral band shape as a result of a decrease of populated vibronic levels. The final shift depends on the ratio of both effects for the same solvent. From the measurements of the compounds in the series **c** in 2-MTHF is evident (Table 2) that the absorption maxima at 77K (detected from fluorescence excitation spectra at 77K) are somewhat bathochromically shifted in comparison with those at room temperature, i.e. an increasing of solvent density at 77 K is decisive.

#### 4.2. Fluorescence spectra

The fluorescence spectra of studied chromophores feature a single band (Fig. 27). Its position depends on the substituent and,

in contrary to absorption spectra, dramatically on the solvent polarity. The solvent dependence of the fluorescence maxima arises from different charge distribution within  $S_0$  and  $S_1$  states at the excited-state equilibrium geometry. In non polar solvents such as DBE, the Stokes shifts are affected by the substituent only negligibly. However, the Stokes shifts are significantly pronounced in polar solvents. The largest shifts were found for the chromophores **2** in MeCN. The influence of solvent polarity on Stokes shifts is small for chromophore series **a**, larger for chromophore series **b** and most pronounced for chromophore series **c** (especially for **2c**).

The fluorescence maxima of chromophores in the series **a** are practically not influenced by solvent polarity – there are small differences between the dipole moments of  $S_0$  and  $S_1$  states and consequently, both states are solvated to a similar extent. For chromophores in the series **b**, a small bathochromic shifts are evident owing to larger differences between  $S_0$  and  $S_1$  dipole

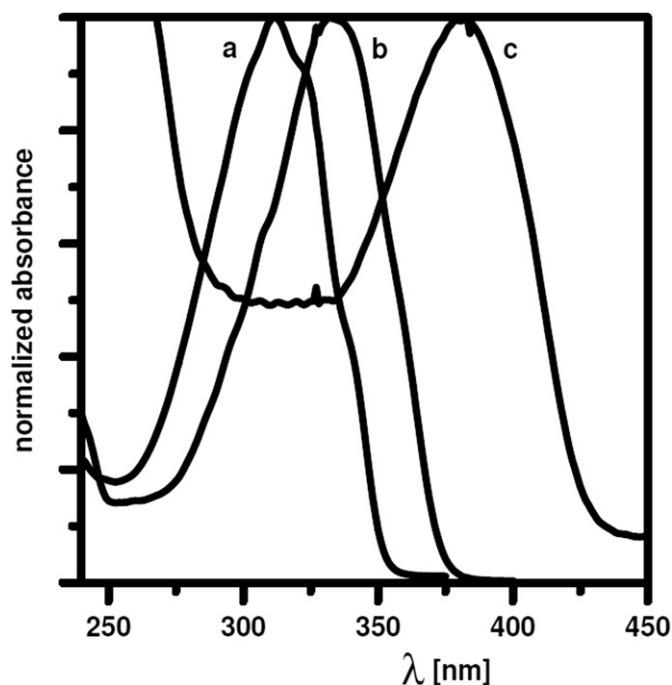


Fig. 4. Absorption spectra of **3a–c** in DBE.

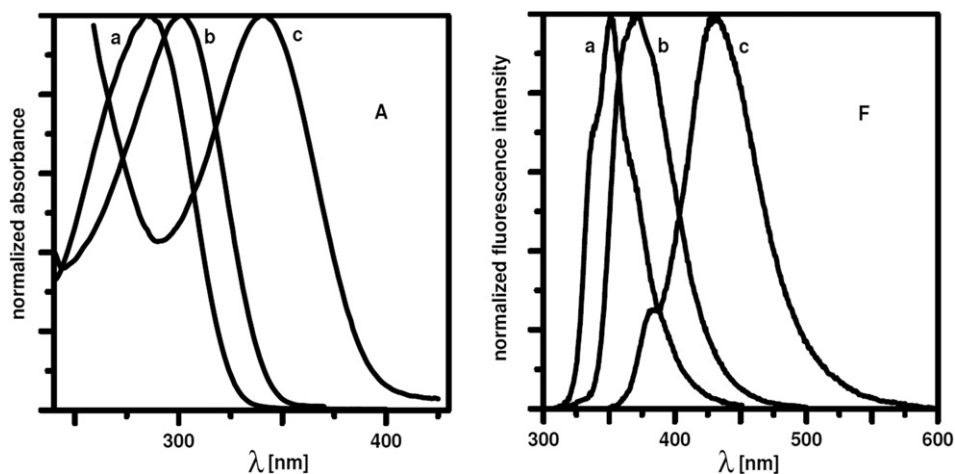


Fig. 5. Absorption (A) and fluorescence (F) spectra of **4a–c** in DBE.

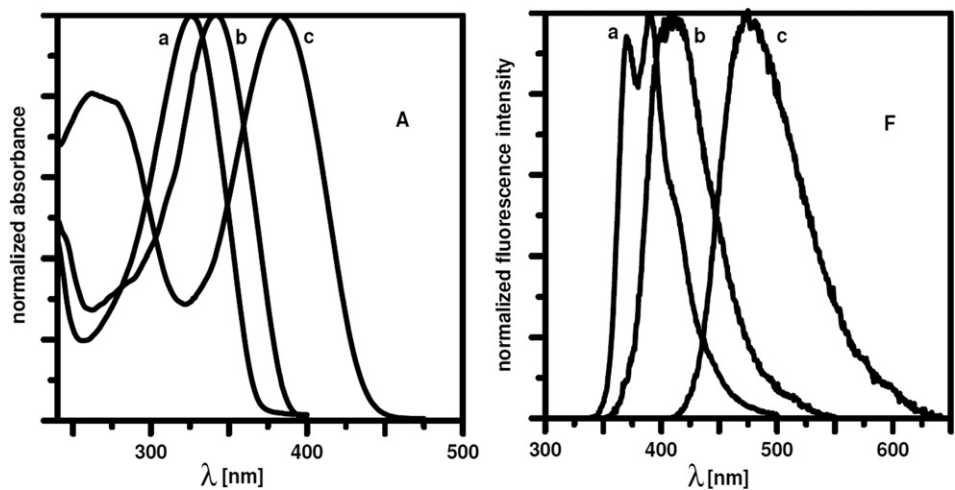


Fig. 6. Absorption (A) and fluorescence (F) spectra of **5a–c** in DBE.

moments. A significant bathochromic shifts were observed for chromophores in the series **c**. These results show that the chromophores in the series **b** and **c** fluoresce from a more or less strongly polar relaxed excited state.

In contrast to absorption maxima, the fluorescence bands were strongly shifted hypsochromically by cooling to 77 K in 2-MTHF (Table 2). This resulted in a strong decrease of Stokes shifts at low temperature. These results show a strong stabilization of the  $S_1$

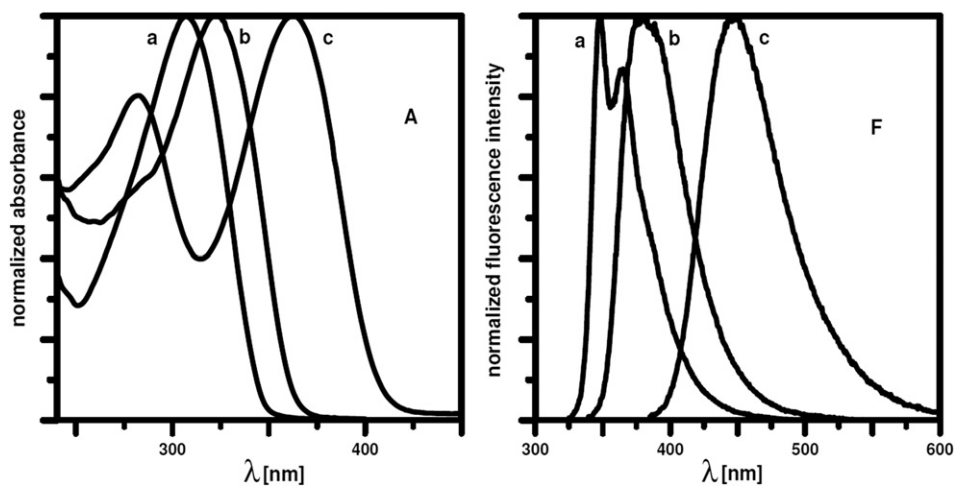


Fig. 7. Absorption (A) and fluorescence (F) spectra of **6a–c** in DBE.

**Table 1**

Absorption and fluorescence maxima (nm) and the Stokes shifts ( $\Delta$ ,  $10^3 \text{ cm}^{-1}$ ) for chromophores **1–6**

Chrom.	DBE			EtAc			MeCN		
	$\lambda^A$	$\lambda^F$	$\Delta$	$\lambda^A$	$\lambda^F$	$\Delta$	$\lambda^A$	$\lambda^F$	$\Delta$
<b>1a</b>	246	—*	—	253	—	—	250	—	—
<b>1b</b>	265	—	—	266	—	—	270	—	—
<b>1c</b>	284	350	6.60	291	361	6.66	296	373	6.97
<b>2a</b>	263	324	7.16	262	320	6.92	260	337	8.79
<b>2b</b>	279	345	6.86	271	354	8.65	264	381	11.63
<b>2c</b>	320	401	6.31	319	452	9.22	315	539	13.19
<b>3a</b>	312	—	—	310	—	—	309	—	—
<b>3b</b>	334	—	—	322	—	—	331	—	—
<b>3c</b>	383	—	—	383	470	4.83	383	470	4.83
<b>4a</b>	285	351	6.60	283	351	6.85	281	354	7.34
<b>4b</b>	301	373	6.41	300	388	7.56	296	419	9.92
<b>4c</b>	341	430	4.07	341	485	8.71	340	—	—
<b>5a</b>	326	390	5.03	325	390	5.13	324	396	5.61
<b>5b</b>	342	410	4.85	339	425	5.97	337	447	7.30
<b>5c</b>	382	475	5.12	381	528	7.31	381	551	8.10
<b>6a</b>	307	364	5.10	304	361	5.19	304	364	5.42
<b>6b</b>	322	378	4.60	319	396	6.10	318	420	7.64
<b>6c</b>	362	445	5.15	360	515	8.36	359	545	9.51

state of chromophores in the series **c** during the life time of the excited state at room temperature. Fluorescence maxima in 2-MTHF at 77 K correspond to the transition from the nuclear equilibrium  $S_1$  state solvated by solvent cage oriented according the ground-state dipole. At room temperature, a further stabilization of  $S_1$  state takes place by reorientation of solvent according  $S_1$  dipole moment and by changing the geometry. These changes are expected to be important with regard to dihedral angles in the chromophore molecular structures. The relatively small fluorescence shift was found for **3c** by cooling, i.e. for the molecule for which a high planarity could be supposed [10].

#### 4.3. Fluorescence quantum yield

While the dependence of Stokes shifts on the chromophore structure and solvent polarity can be interpreted, an unambiguous relationship have not been found for fluorescence quantum yield  $q_F$  (Table 3). Chromophores **1** and **3** showed a very low or no fluorescence. Chromophores **4a,b** and **6a,b** in all used solvents as well as chromophores in the series **c** in DBE and EtAc showed fluorescence with high  $q_F$ . Chromophore **5a** in all solvents and **5c** in DBE and EtAc showed a strong fluorescence, while a relatively high fluorescence was observed for **2b** in all solvents and for **2c** in DBE and EtAc. Compared to **2b** and **5b**, a very low  $q_F$  was measured for **2a** in acetonitrile and for **5b** in all other solvents. No fluorescence was found for chromophores in the series **c** in ethanol. As the fluorescence intensity was not corrected for the refractive index and the solvent volume contraction at 77 K, the temperature effect on the fluorescence intensity for chromophores in the series **c** measured in 2-MTHF could be estimated only relatively. Upon cooling the chromophore solutions to 77 K, the fluorescence intensity raised by

**Table 2**

The absorption ( $\lambda^A$ ) and fluorescence ( $\lambda^F$ ) maxima (nm) and the Stokes shifts ( $\Delta$ ,  $10^3 \text{ cm}^{-1}$ ) of the series **c** in 2-methyltetrahydrofuran (2-MTHF) at room temperature (RT) and at 77 K (LT).

No	$\lambda_{RT}^A$	$\lambda_{RT}^F$	$\Delta_{RT}$	$\lambda_{LT}^A$	$\lambda_{LT}^F$	$\Delta_{LT}$
<b>2c</b>	320	438	8.42	320	400	6.25
<b>3c</b>	383	461	4.42	393	437	2.56
<b>4c</b>	344	480	8.24	346	414	4.75
<b>5c</b>	385	523	6.85	389	455	3.73
<b>6c</b>	363	508	7.86	380	424	2.73

**Table 3**

Measured fluorescence quantum yields.

No.	DBE	EtAc	MeCN
<b>1a</b>	—	—	—
<b>1b</b>	—	—	—
<b>1c</b>	0.02	0.05	0.02
<b>2a</b>	0.26	0.28	0.01
<b>2b</b>	0.50	0.65	0.35
<b>2c</b>	0.52	0.37	0.08
<b>3a</b>	—	—	—
<b>3b</b>	—	—	—
<b>3c</b>	—	0.04	0.02
<b>4a</b>	0.72	0.87	0.93
<b>4b</b>	0.80	0.98	0.27
<b>4c</b>	0.75	0.64	—
<b>5a</b>	0.62	0.59	0.41
<b>5b</b>	0.20	0.15	0.12
<b>5c</b>	0.30	0.53	<0.01
<b>6a</b>	0.73	0.80	0.76
<b>6b</b>	0.70	0.83	0.63
<b>6c</b>	0.85	0.73	0.05

about 10–20% for **3c**, **4c** and **5c**, i.e. for the compounds with two or three dihedral angles. Only small differences have been observed for **2c** and **6c**.

As a main feature, a strong fluorescence quench was observed for chromophores in the series **c** measured in polar solvents. Fig. 8 shows the relation between the  $q_F$  and  $\lambda_{\text{max}}^F$  versus the different mixtures of non polar DBE and strongly polar acetonitrile for the chromophore **2c**. These dependencies demonstrate a decrease of relative  $q_F$  with the bathochromic shift of the fluorescence maxima in polar environment. No dual fluorescence was found. The increase of radiationless decay rate constant with the fluorescence bathochromic shift is successive and regulated by the classical “energy gap law” [19]. Hence, an efficient solvent dependent nonradiative process (probably  $S_1$ – $S_0$  internal conversion) could be responsible for the fluorescence quenching of chromophores in the series **c** measured in polar solvents.

#### 4.4. Theoretical results

The dihedral angles for the studied chromophores in optimized geometries (AM1) are presented in Table 4. A small influence of the R-substituent on the chromophore geometry is obvious. The angle ( $\alpha$ ) between the phenyl ring and the DCI moiety is the same for compounds **2**, **4**, **5**, **6**, i.e.  $44 \pm 1^\circ$ . The DCI moiety and terminal phenyl ring are mutually almost planar for all chromophores **4** and **5**, the central 1,4-phenyl ring is distorted by  $41$ – $47^\circ$  depending on a substituent. The phenyl rings attached to ethynylene moiety (**6**) are mutually coplanar. Chromophores **3** exhibit a relative planarity between the DCI moiety and the double bond; chromophore **3c** is almost planar. These results correspond with the crystallographic data [10].

Theoretical spectral characteristics of the first two optical transitions for the optimized geometry of the studied chromophores are shown in Table 5. The first transition corresponds to the transition from the electronic ground-state  $S_0$ – $S_1(\pi\pi^*)$  excited state with the main mono-excited configuration HOMO–LUMO and with a high oscillator strength. An agreement of theoretical values with experimental  $\lambda_{\text{max}}^A$  is satisfactory, though the theoretical transitions are shifted bathochromically for chromophores in the series **a** and hypsochromically for the series **c**. The second optical transition, corresponding to  $S_0$ – $S_3$  or to  $S_0$ – $S_4 \pi\pi^*$  transitions with the main configuration HOMO–LUMO+1 is predicted to be in region 250–290 nm for all studied chromophores. The corresponding absorption band is observable on the absorption spectra



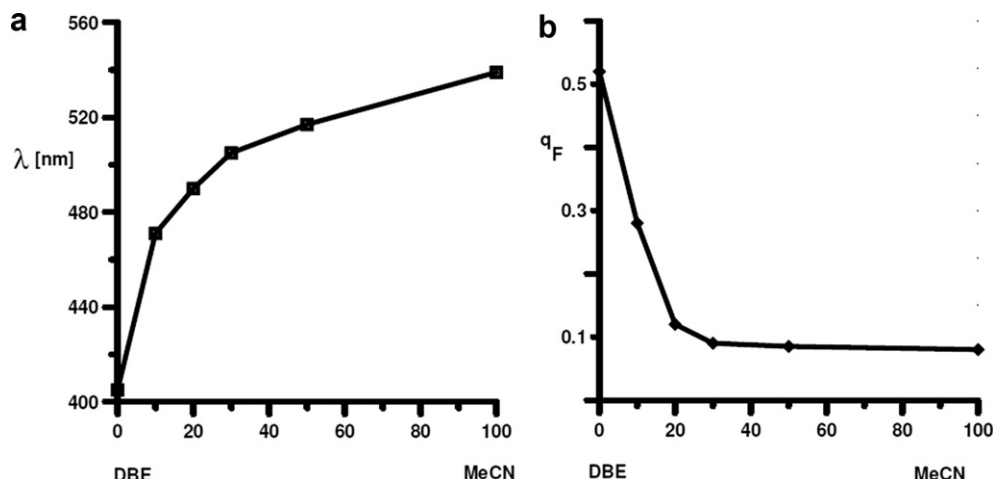


**Fig. 8.** The dependence of the fluorescence maxima (a) and the fluorescence quantum yields (b) for **2c** on the solvent polarity represented by a various mixtures of acetonitrile and DBE.

of **5c** and **6c** (Fig. 6A and 7A). In the case of the other chromophores, the intense first absorption band could overlap this band or it appears as a shoulder on the absorption spectrum. However, the results of fluorescence anisotropy measurements for **2c** and **6b** (Fig. 9) revealed two overlapped bands in the region of 280–310 nm. The other transitions have a very low oscillator strength and/or are strongly mixed and probably do not influence the spectral and photophysical properties of studied compounds.

The HOMO orbitals of all chromophores showed the same character: a) a localization on the rings, on multiple bonds (**3** and **5**) and on substituents; b) a nodal plane between the rings mutually and between the rings and multiple bonds. The LUMO orbitals showed a strong  $\pi$ -interaction between the rings (**2**, **4** and **6**) and between the rings and multiple bonds (**3** and **5**); at the same time, a  $\pi$ -character of originally double bond was strongly reduced; it enables a rotation around these bonds in the first excited state resulting in *E*–*Z* isomerization of chromophores **3** and **5** [20]. Depending on the character of substituents, the LUMO orbitals are more or less delocalized (chromophores in the series **a** and **b**); a strong localization on the DCI moiety was found for chromophores in the series **c**.

The HOMO–LUMO transition is connected with a weak CT from hydrocarbon subunit to the DCI moiety for the chromophores in the series **a** and **b**. A very strong CT was found for the chromophores in the series **c**: from dimethylaminophenyl to DCI (**2c**), from dimethylaminophenyl to DCI-phenyl (**4c**), from dimethylaminostilbenyl

to DCI-phenyl (**5c**) and from  $-\text{C}\equiv\text{C}$ -phenyldimethylamino moiety to DCI-phenyl subsystem (**6c**). Relatively weak CT in  $S_1$  state and a strong CT in  $S_2$  state (from dimethylaminostyryl subunit to DCI) were found for **3c**.

**Table 5**  
Theoretical spectral characteristics of  $S_0$ – $S_1$  transitions.

No.	State	$\lambda^{\text{theor}}$ [nm]	$f$	Main CI configuration	DM (Debye)		$\lambda^{\text{exp}}$ [nm] (in DBE)
					Exc. st.	G. st.	
<b>1a</b>	1.	281	0.371	24–25 (0.94)	9.4	8.7	246
	3.	252	0.051	24–26 (0.87)	6.8		
<b>1b</b>	1.	290	0.385	30–31 (0.95)	9.3	7.7	265
	3.	258	0.092	30–32 (0.83)	5.6		
<b>1c</b>	1.	293	0.394	33–34 (0.95)	10.4	8.6	284
	3.	261	0.126	33–35 (0.89)	7.3		
<b>2a</b>	1.	299	0.599	38–39 (0.96)	8.0	9.5	263
	3.	272	0.213	38–40 (0.82)	9.5		
<b>2b</b>	1.	302	0.684	44–45 (0.96)	8.6	8.9	279
	3.	273	0.260	44–46 (0.87)	9.8		
<b>2c</b>	1.	312	0.803	47–48 (0.90)	13.6	10.8	320
	3.	277	0.326	47–49 (0.81)	14.5		
<b>3a</b>	1.	336	1.153	43–44 (0.97)	7.7	9.9	312
	3.	287	0.186	43–45 (0.81)	13.9		
<b>3b</b>	1.	343	1.239	49–50 (0.97)	10.0	10.7	334
	3.	287	0.187	49–51 (0.87)	15.2		
<b>3c</b>	1.	356	1.344	52–53 (0.95)	14.2	11.5	383
	3.	291	0.211	52–54 (0.82)	11.5		
<b>4a</b>	1.	306	0.961	52–53 (0.93)	9.2	9.9	285
	4.	275	0.340	52–54 (0.78)	11.7		
<b>4b</b>	1.	309	1.070	58–59 (0.89)	9.6	9.0	301
	4.	276	0.398	58–60 (0.78)	12.5		
<b>4c</b>	1.	315	1.247	61–62 (0.74)	15.0	11.4	341
	4.	281	0.346	61–63 (0.62)	17.4		
<b>5a</b>	1.	323	1.489	60–62 (0.60)	11.4	10.1	326
	3.	284	0.688	57–59 (0.69)	13.2		
<b>5b</b>	1.	329	1.595	56–58 (0.51)	12.3	9.3	342
	4.	286	0.396	63–64 (0.88)	12.9		
<b>5c</b>	1.	339	1.687	62–64 (0.60)	17.8	11.8	382
	4.	292	0.274	63–65 (0.63)	15.4		
<b>6a</b>	1.	320	1.594	65–67 (0.67)	17.2	11.4	362
	3.	280	0.444	66–68 (0.51)	14.0		
<b>6b</b>	1.	324	1.709	56–57 (0.90)	11.3	10.0	307
	4.	283	0.401	56–58 (0.74)	14.0		
<b>6c</b>	1.	331	1.854	62–63 (0.87)	12.2	9.5	322
	4.	287	0.283	62–64 (0.66)	13.7		
	1.	331	1.854	61–63 (0.55)	17.2	11.4	362
	4.	287	0.283	65–66 (0.79)	15.7		
	1.	331	1.854	64–66 (0.66)	15.7		
	4.	287	0.283	65–67 (0.55)			

**Table 4**  
The dihedral angles of chromophores **1–6** in optimized geometries (AM1).

No.	$\alpha$	$\beta$
<b>2a</b>	43	
<b>2b</b>	44	
<b>2c</b>	44	
<b>3a</b>	3	20
<b>3b</b>	3	17
<b>3c</b>	4	13
<b>4a</b>	44	41
<b>4b</b>	44	40
<b>4c</b>	44	40
<b>5a</b>	44	23
<b>5b</b>	44	23
<b>5c</b>	45	23
<b>6a</b>	44	
<b>6b</b>	45	
<b>6c</b>	45	

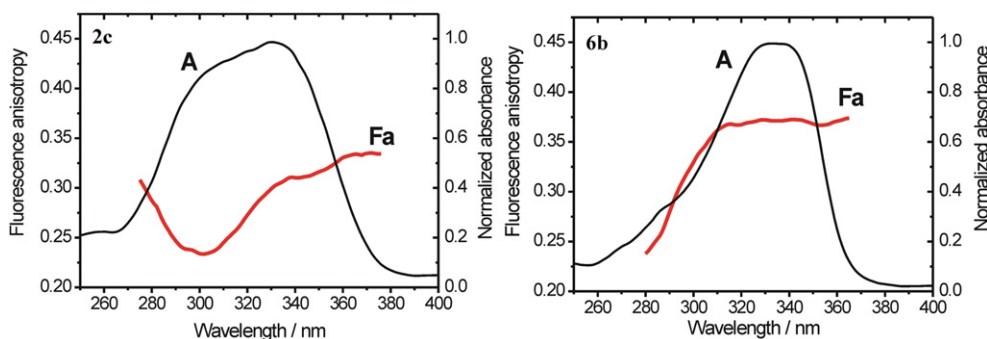


Fig. 9. Absorption (A) and fluorescence anisotropy (Fa) spectra of **2c** and **6b** in 2-MTHF at 130 K.

The experimental results show that geometry changes occurring during a relaxation process play an important role in deactivation mechanism of excited states of studied compounds. As the excited states are not geometry optimized (corresponding software is not generally available), we have investigated a character of vertically excited states for different geometries of the ground state. Regarding the existence of more dihedral angles, the problem of a choice of their mutual combination is rather complicated. Therefore, the investigation has been performed only for chromophores **2**, i.e. the substance with only one dihedral angle ( $\alpha$ ). We have calculated the spectral characteristics for  $\alpha = 0^\circ$  (planar geometry),  $44^\circ$  (optimized geometry),  $60^\circ$  and  $90^\circ$ .

For chromophore **2a**, we have found:

- independently on  $\alpha$ , the first transition retains HOMO–LUMO character,
- with increasing  $\alpha$ ,  $\lambda_{\max}^A$  shifts hypsochromically (from 316 nm to 286 nm),
- oscillator strength is reduced and dipole moment of the first excited state raises (from 6.7 D to 10.4 D), the ground-state dipole moment is 9.5 D for all structures;

For chromophore **2c**, we have found:

- the first transition retains HOMO–LUMO character for  $\alpha = 0^\circ$ – $60^\circ$ ; at the same time,  $\lambda_{\max}^A$  shifts hypsochromically (from 332 nm to 302 nm) and oscillator strength is somewhat reduced,
- dipole moment of the first excited state raises from 12.8 D to 14.4 D and that of ground state somewhat sinks (from 11.3 D to 10.1 D) for  $\alpha$  from  $0^\circ$  to  $90^\circ$ ,
- for dihedral angle  $90^\circ$ , the first two transitions are localized on acceptor and donor moieties, respectively, and their transition dipole moments are very close to the ground-state dipole moment (10.4 D), only the third transition exhibits a strong CT character (dipole moment 21 D) and is mixed from HOMO–LUMO and HOMO–LUMO+1 transitions;  $\lambda_{\max}^A$  is strongly shifted hypsochromically to 260 nm and oscillator strength is reduced from 0.910 for planar structure to 0.315.

The solvent polarity and temperature effect on fluorescence characteristics, together with theoretical results, may prove the studied chromophores aim at more or less planar geometry within the course of relaxation process of the first excited state.

## 5. Conclusion

The substitution and the solvent polarity affect the positions of the absorption and fluorescence maxima and the fluorescence

quantum yields most significantly. Replacement of the hydrogen atom in chromophore series **a** by an electron donor groups as in the series **b** and **c**, led to a bathochromic shift of the first absorption band. Whereas the position of the absorption maxima was not influenced by the increasing solvent polarity, the fluorescence maxima of chromophores in the series **c** were shifted strongly bathochromically. Simultaneously, a significant decrease of  $q_F$  was observed. In contrast to the measured absorption maxima, the fluorescence bands were shifted strongly hypsochromically by cooling to 77 K in 2-MTHF. These experimental results showed that geometry changes play an important role in position of the fluorescence maxima and consequently in deactivation mechanism of the first excited state. An efficient solvent dependent nonradiative process (probably  $S_1$ – $S_0$  internal conversion) could be responsible for the fluorescence quenching for chromophores in the series **c** measured in polar solvents.

A small impact of the R-substituent on the optimized geometry (AM1) was found. Chromophores in the series **c**, **3c** in particular, exhibited a relatively high planarity, the other compounds are more or less distorted. The first theoretical transition (INDO/S) for all compounds corresponds to  $S_0$ – $S_1$  ( $\pi\pi^*$ ) transition with main mono-excited configuration HOMO–LUMO accompanied by a strong charge transfer and a high transition dipole moment for chromophores in the series **c**. The calculated transition energies correspond with the experimental data.

## Acknowledgements

The financial support from the Czech Ministry of Education Youth and Sports (grant VZ MSM No 0021627501) is acknowledged.

## References

- [1] Forrest SR, Thompson ME. Special issue on “Organic electronic and optoelectronics”. *Chem Rev* 2007;107(4):923–1386.
- [2] Apent P, Rasmussen PG. Synthesis and properties of new derivatives of 4,5-dicyanoimidazole and 4,4',5,5'-tetracyano-2,2'-biimidazole. *J Am Chem Soc* 1991;113(16):6178–87.
- [3] Shin RY, Sonar P, Siew PS, Chen ZK, Sellinger A. Electron-accepting conjugated materials based on 2-vinyl-4,5-dicyanoimidazoles for application in organic electronics. *J Org Chem* 2009;74(9):3293–8.
- [4] Carella A, Centore R, Sirigu A, Tuzi A, Quatela A, Schutzmann S, et al. Second order nonlinear optical performances of polymers containing imidazole and benzimidazole chromophores. *Macromol Chem Phys* 2004;205:1948–54.
- [5] Carella A, Centore R, Riccio P, Sirigu A, Quatela A, Palazzesi Ch, et al. Poly-methacrylate copolymers containing 4,5-dicyanoimidazole-based chromophores and their nonlinear optical behavior. *Macromol Chem Phys* 2005;206:1399–404.
- [6] Bureš F, Pytela O, Diederich F. Solvent effects on electronic absorption spectra of donor-substituted 11,11,12,12-tetracyano-9,10-anthraquinodimethanes (TCAQs). *J Phys Org Chem* 2009;22(2):155–62.
- [7] Bureš F, Pytela O, Kivala M, Diederich F. Solvatochromism as an efficient tool to study *N,N*-dimethylamino- and cyano-substituted  $\pi$ -conjugated molecules

- with an intramolecular charge-transfer absorption. *J Phys Org Chem*; 2010. doi:10.1002/poc.1744.
- [8] Bureš F, Schweizer WB, May JC, Boudon C, Gisselbrecht JP, Gross M, et al. Property tuning in charge-transfer chromophores by systematic modulation of the spacer between donor and acceptor. *Chem Eur J* 2007;13(19): 5378–87.
- [9] Wu YL, Bureš F, Jarowski PD, Schweizer WB, Boudon C, Gisselbrecht JP, et al. Proaromaticity: organic charge-transfer chromophores with small HOMO–LUMO gaps. *Chem Eur J* 2010;16(31):9592–605.
- [10] Kulhánek J, Bureš F, Pytela O, Mikysek T, Ludvík J, Růžicka A. Push–pull molecules with a systematically extended  $\pi$ -conjugated system featuring 4,5-dicyanoimidazole. *Dyes Pigm* 2010;85(1–2):57–65.
- [11] Bureš F, Kulhánek J, Mikysek T, Ludvík J, Lokaj J. Branched charge-transfer chromophores featuring a 4,5-dicyanoimidazole unit. *Tetrahedron Lett* 2010; 51(15):2055–8.
- [12] Kulhánek J, Bureš F, Mikysek T, Ludvík J, Pytela O. Imidazole as a central  $\pi$ -linkage in Y-shaped push–pull chromophores. *Dyes Pigm* 2010;90(1): 48–55.
- [13] Kulhánek J, Bureš F, Wojciechowski A, Makowska-Janusik M, Gondek E, Kityk IV. Optical operation by chromophores featuring 4,5-dicyanoimidazole embedded within poly(methyl methacrylate) matrices. *J Phys Chem A* 2010; 114(35):9440–6.
- [14] Berlman IB. Handbook of fluorescence spectra of aromatic molecules. New York: Academic Press; 1965.
- [15] Birks JB, Dyson DJ. The relations between the fluorescence and absorption properties of organic molecules. *Proc Royal Soc* 1963;A275:135–48.
- [16] Jones II G, Rahman MA. Fluorescence properties of coumarin laser dyes in aqueous polymer media. chromophore isolation in poly(methacrylic acid) hypercoils. *J Phys Chem* 1994;98:13028–37.
- [17] Thompson MA. ArgusLab 4.0, vol. 29. Seattle, WA: Planaria Software LLC, <http://www.arguslab.com>; 2009.
- [18] Mataga N, Kubota T. Molecular interactions and electronic spectra. New York: Marcel Dekker, Inc.; 1970. p. 122.
- [19] Avouris P, Gelbard WM, El-Sayed MA. Nonradiative electronic relaxation under collision-free conditions. *Chem Rev* 1977;77(6):793–833.
- [20] Almonasy N. Unpublished results.